Phase transition properties of rotating Quark-Gluon-Plasma.

Pracheta Singha

Victor E. Ambrus, Maxim N. Chernodub.

Phys.Rev.D 110 (2024) 9, 094053

ZIMÁNYI SCHOOL 2024

Table of Contents

Motivation

- Properties of Quark-Gluon-Plasma (QGP):
  - Underlying symmetries.
  - equation of state and medium thermodynamics.
  - Phase structure.

In the presence of :

  - finite temperature (T).
  - finite chemical potential (μ).
  - finite rotation (Ω).

Motivation

- Properties of Quark-Gluon-Plasma (QGP):
  - Underlying symmetries.
  - equation of state and medium thermodynamics.
  - Phase structure.

In the presence of :

- finite temperature (T).
- finite chemical potential (μ).
- finite rotation (Ω).

Motivation

- Angular momentum in noncentral collisions $\approx 1000\hbar \implies$ A strong vortical structure of the resulting fluid.

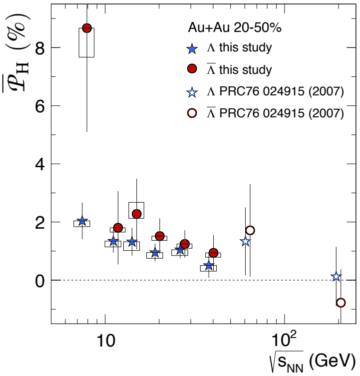

Figure 1: The hyperon average polarization in Au-Au collision . STAR collaboration. Nature 548, 62–65 (2017)

- $\bar{\mathcal{P}}_{\mathrm{H}} \equiv \langle \mathcal{P}_H \cdot \hat{J}_{\mathrm{sys}} \rangle$
- $\hat{J}_{\mathrm{sys}} \equiv$ Direction of the angular momentum of the collision.
- $\mathcal{P}_{\mathrm{H}} \equiv$ Hyperon polarization vector in the hyperon rest frame.
- The Fluid vorticity can be estimated from the data $\implies$ "most vortical fluid produced in the laboratory" .

STAR collaboration. Nature 548, 62–65 (2017)

Becattini et al, Phys. Rev. C 95, 054902, (2017)

STAR collaboration. Phys.Rev.C76:024915 (2007)

Motivation

- Presence of vorticity in the system will affect the thermodynamic properties and the phase structure of the QGP.

- Lattice result : Increasing angular velocity increases the transition temperature. Braguta et al. Phys. Rev. D 103, 094515 (2021) , Ji-Chong Yang et al arXiv:2307.05755 [hep-lat]

- Effective model studies: without boundary condition:

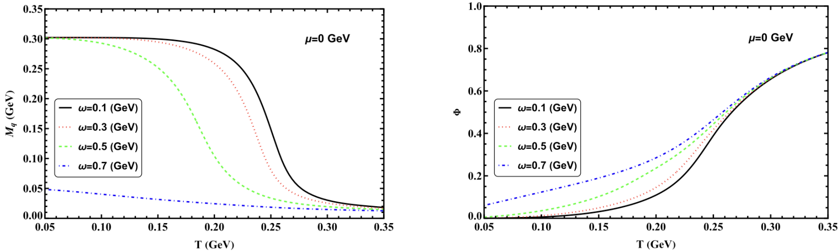

Figure 2: Temperature variation of effective quark mass and traced Polyakov loop. Mei Huang et al, PhysRevD.108.096007, (2023)

Motivation

- Presence of vorticity in the system will affect the thermodynamic properties and the phase structure of the QGP.

- Lattice result : Increasing angular velocity increases the transition temperature. Braguta et al. Phys. Rev. D 103, 094515 (2021) , Ji-Chong Yang et al arXiv:2307.05755 [hep-lat]

- Effective model : Increasing angular velocity decreases the transition temperature.

- Objective 1 :

The chiral and deconfinement phase transitions in a rotating Bounded system.

Motivation : Tolman Ehrenfest analogy

- Rigid rotation with constant angular velocity Ω around z axis:

$$T_{\mathrm{TE}}(\rho) = \frac{T_0}{\sqrt{1 - \Omega^2 \rho^2}}$$

TE Prediction : Deconfinement starts at the peripheral region and approaches the center.

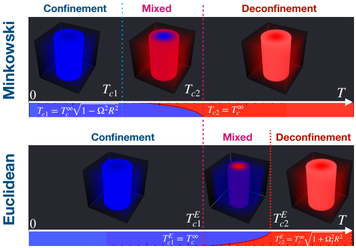

Figure 2: TE prediction. PhysRevD.107.114502

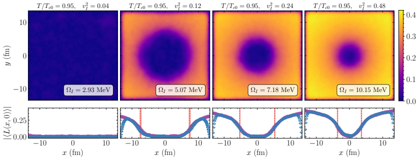

Figure 3: Lattice results.Phys.Lett.B 855 (2024), 138783

Motivation : Tolman Ehrenfest analogy

- Rigid rotation with constant angular velocity Ω around z axis:

$$T_{\mathrm{TE}}(\rho) = \frac{T_0}{\sqrt{1 - \Omega^2 \rho^2}}$$

TE Prediction : Deconfinement starts at the peripheral region and approaches the center.

Lattice result : Deconfinement starts at the center and approaches the boundary.

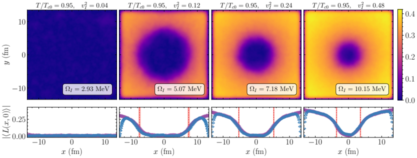

Figure 2: Lattice results. Phys.Lett.B 855 (2024), 138783

Motivation : Tolman Ehrenfest analogy

TE Prediction : Deconfinement starts at the peripheral region and approaches the center.

Lattice result : Deconfinement starts at the center and approaches the boundary.

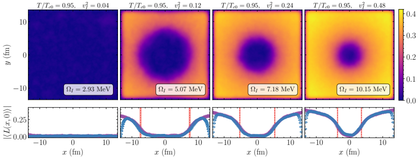

Figure 2: Lattice results. Phys.Lett.B 855 (2024), 138783

- Objective 2 :

Does the Tolman-Ehrenfest analogy hold for a rotating bounded system?

Polyakov Linear Sigma model with Quarks

- Model Lagrangian:

$$\mathcal{L}(\phi, \psi, L) = \mathcal{L}_{\mathcal{M}}(\phi) + \mathcal{L}_q(\phi, \psi, L) + \mathcal{L}_L(L)\,.$$

- Mesonic contribution:

$$\mathcal{L}_{\mathcal{M}}(\phi) = \frac{1}{2}\left(\partial_\mu \sigma \partial^\mu \sigma + \partial_\mu \vec{\pi} \partial^\mu \vec{\pi}\right) - V_{\mathcal{M}}(\sigma, \vec{\pi})\,,$$

$$V_{\mathcal{M}}(\sigma, \vec{\pi}) = \frac{\lambda}{4}\left(\sigma^2 + \vec{\pi}^2 - v^2\right)^2 - h\sigma\,.$$

- Quark contribution:

$$\mathcal{L}_q = \bar{\psi}\left(i\not{D} - g\phi\right)\psi \equiv \bar{\psi}\left[i\not{D} - g(\sigma + i\gamma_5 \vec{\tau} \cdot \vec{\pi})\right]\psi$$

Polyakov Linear Sigma model with Quarks

- Mesonic contribution:

$$\mathcal{L}_{\mathcal{M}}(\phi) = \frac{1}{2}\left(\partial_\mu \sigma \partial^\mu \sigma + \partial_\mu \vec{\pi} \partial^\mu \vec{\pi}\right) - V_{\mathcal{M}}(\sigma, \vec{\pi}) \,,$$
$$V_{\mathcal{M}}(\sigma, \vec{\pi}) = \frac{\lambda}{4}\left(\sigma^2 + \vec{\pi}^2 - v^2\right)^2 - h\sigma \,.$$

- Quark contribution:

$$\mathcal{L}_q = \bar{\psi}\left(i\not{D} - g\phi\right)\psi \equiv \bar{\psi}(i\not{D})\psi - g\bar{\psi}(\sigma + i\gamma_5 \vec{\tau}\cdot\vec{\pi})\psi$$

- $h\sigma \equiv$ explicit chiral symmetry breaking $\rightarrow m_\pi \neq 0$.
- Model parameters: $\lambda,\ v,\ g,\ h$, are fixed by $m_\pi,\ f_\pi,\ m_\sigma,\ m_q$.

Polyakov Linear Sigma model with Quarks

- Mesonic contribution:

$$\mathcal{L}_{\mathcal{M}}(\phi) = \frac{1}{2}\left(\partial_\mu \sigma \partial^\mu \sigma + \partial_\mu \vec{\pi} \partial^\mu \vec{\pi}\right) - V_{\mathcal{M}}(\sigma, \vec{\pi}),$$
$$V_{\mathcal{M}}(\sigma, \vec{\pi}) = \frac{\lambda}{4}\left(\sigma^2 + \vec{\pi}^2 - v^2\right)^2 - h\sigma .$$

- Quark contribution:

$$\mathcal{L}_q = \bar{\psi}\left(i\not{D} - g\phi\right)\psi \equiv \bar{\psi}\left[i\not{D} - g(\sigma + i\gamma_5 \vec{\tau}\cdot\vec{\pi})\right]\psi$$

- Polyakov contribution:

$$\frac{\mathcal{L}_L}{T^4} = \frac{a(T)L^* L}{2} - b(T)\ln\left[1 - 6L^*L + 4\left(L^{*3} + L^3\right) - 3(L^*L)^2\right]$$

Thermodynamic potential

- Thermodynamic potential:

$$Z = \mathrm{Tr}\left(\mathrm{e}^{-\beta(H-\mu N)}\right)$$

$$F(T) = -\frac{T\ln\mathcal{Z}}{V} = V_{\mathcal{M}} + V_L + F_{\psi\bar{\psi}}$$

where,

$$F_{\psi\bar{\psi}} = -2N_f T\sum_{\varsigma=\pm1}\int\frac{d^3p}{(2\pi)^3}F_\varsigma\,.$$

$$F_+ = \ln\left[1 + 3Le^{-\beta\mathcal{E}_+} + 3L^* e^{-2\beta\mathcal{E}_+} + e^{-3\beta\mathcal{E}_+}\right],$$

$$F_- = \ln\left[1 + 3L^* e^{-\beta\mathcal{E}_-} + 3Le^{-2\beta\mathcal{E}_-} + e^{-3\beta\mathcal{E}_-}\right].$$

Thermodynamic potential

- Thermodynamic potential:

$$Z = \mathrm{Tr}\left(\mathrm{e}^{-\beta(H-\mu N)}\right)$$

$$F(T) = -\frac{T\ln\mathcal{Z}}{V} = V_{\mathcal{M}} + V_L + F_{\psi\bar{\psi}}$$

- Saddle point equations:

$$\frac{\partial(F_{\psi\bar{\psi}} + V_{\mathcal{M}})}{\partial\sigma} = 0\,; \quad \frac{\partial(F_{\psi\bar{\psi}} + V_L)}{\partial L} = 0\,; \quad \frac{\partial(F_{\psi\bar{\psi}} + V_L)}{\partial L^*} = 0$$

- All thermodynamic observables are evaluated from the thermodynamic potential $F(\sigma_{\mathrm{mf}}, L_{\mathrm{mf}}, L^*_{\mathrm{mf}})$

Rotating cylindrical system

- Cylinder of radius R rigidly rotating about the z axis in the counterclockwise direction.
- We assume the effects of rotation on to the quark sector.
- Conservation of angular momentum J_z.
- Causality criteria : $\Omega R \leq 1$.
- Transverse direction is finite $\Longrightarrow$ transverse momentum is discrete.

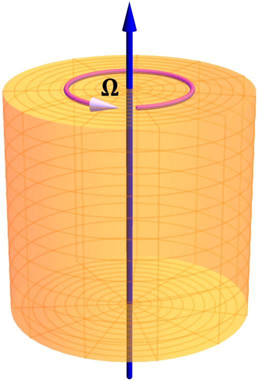

Figure 3: Rigidly rotating cylinder M.N. Chernodub et. al. 10.1007/JHEP01(2017)136.

Modified free energy including rotation

- Quark contribution to the free energy:

$$F_{\psi\bar{\psi}} = -\frac{2N_f T}{\pi R^2}\sum_{l=1}^{\infty}\sum_{m=-\infty}^{\infty}\int\frac{dp_z}{2\pi}\tilde{F}_{\varsigma}\,.$$

$$\tilde{F}_{+} = \ln\left[1 + 3Le^{-\beta\tilde{\mathcal{E}}_{+}} + 3L^{*}e^{-2\beta\tilde{\mathcal{E}}_{+}} + e^{-3\beta\tilde{\mathcal{E}}_{+}}\right],$$

$$\tilde{F}_{-} = \ln\left[1 + 3L^{*}e^{-\beta\tilde{\mathcal{E}}_{-}} + 3Le^{-2\beta\tilde{\mathcal{E}}_{-}} + e^{-3\beta\tilde{\mathcal{E}}_{-}}\right].$$

- Non rotating system $\to$ rotating bounded system:

$$Z \to \mathrm{Tr}\left(\mathrm{e}^{-\beta(H-\mu N-\Omega J_z)}\right);\quad \int\frac{d^3p}{(2\pi)^3} \to \frac{1}{\pi R^2}\sum_{l=1}^{\infty}\sum_{m=-\infty}^{\infty}\int\frac{dp_z}{2\pi}$$

$$\mathcal{E}_{\pm} = \left(p^2 + g^2\sigma^2\right)^{\frac{1}{2}} \mp \mu \to \tilde{\mathcal{E}}_{\pm} = \left(p_z^2 + \frac{\xi_{ml}^2}{R^2} + g^2\sigma^2\right)^{\frac{1}{2}} - \Omega\left(m+\frac{1}{2}\right) \mp \mu$$

Phase Diagram in $T-\mu$ plane

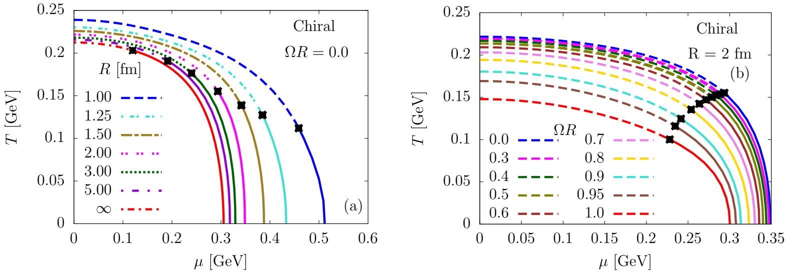

Figure 4: The phase diagram of bounded system for (a) different radii at $\Omega R = 0$ and (b) Different ΩR at radius 2 fm .

- Transition temperature decreases as radius increases.
- Boundary effects drag the critical point towards increasing μ .
- Transition temperature decreases as angular velocity increases.
- Finite rotation drags down the critical point towards decreasing μ .

PHASE DIAGRAM $T - \mu$ PLANE

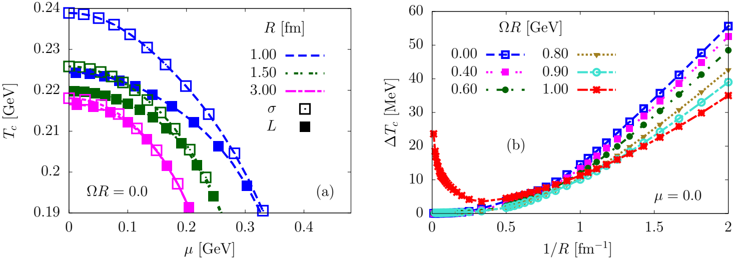

Figure 5: (a) $T - \mu$ Phase diagram for chiral and deconfinement crossovers at $\Omega R = 0$, and (b) difference in chiral and deconfinement phase transition temperature as a function of $1/R$ for different ΩR at $\mu = 0$.

- There is a difference in chiral and deconfinement crossover temperatures, $\Delta T_c = T_c^{(\sigma)} - T_c^{(L)}$.
- The splitting increases as we decrease the radius, chemical potential or angular velocity. PS, V. Ambrus, M. Chernodub. Phys.Rev.D 110 (2024) 9, 094053

Phase diagram $T - \Omega R$ plane

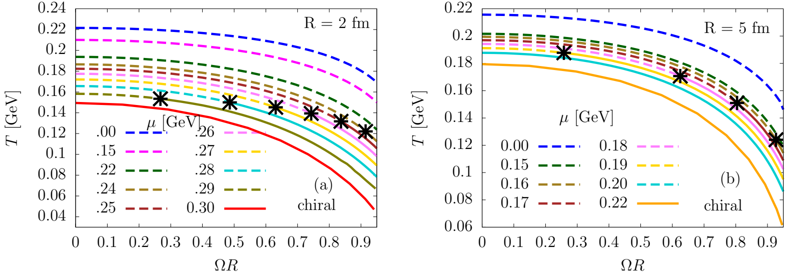

Figure 6: Phase diagram with different chemical potential (a) $R = 2$ fm and (b) $R = 5$ fm.

- As R increases, the range of μ over which there is a critical point decreases.

Phase diagram

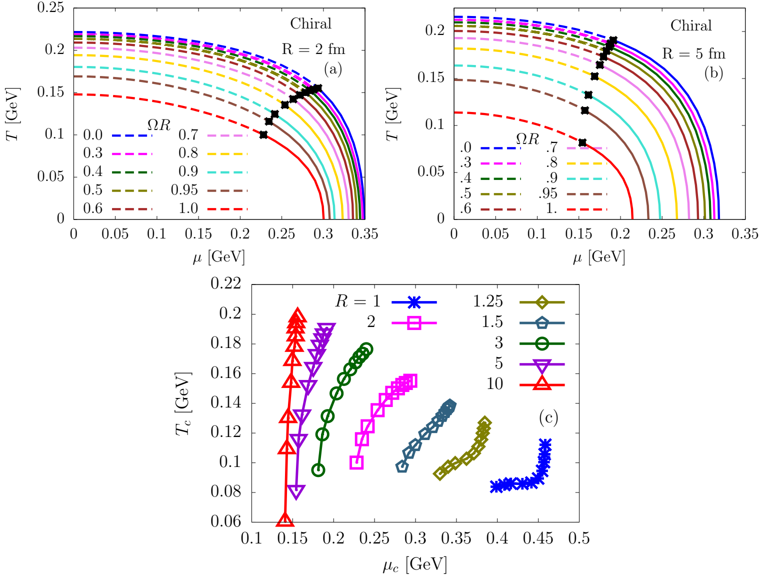

Tolman Ehrenfest analogy :

- Objective: understanding the dependence of T_c on ΩR.
- Saddle point equation : $\lambda(\sigma^2 - v^2) - h - g\langle\bar{\psi}\psi\rangle = 0$
- In the presence of rotation :

$$T_\rho = \Gamma_\rho T, \quad u^\mu \partial_\mu = \Gamma_\rho(\partial_t + \Omega\partial_\varphi), \quad \Gamma_\rho = (1 - \rho^2\Omega^2)^{-1/2}\,.$$

$$\langle\bar{\psi}\psi\rangle_\rho = \frac{3N_f g\sigma}{\pi^2} T_\rho^2 \sum_{\varsigma=\pm 1} \int \frac{dx\, x^2}{y_\rho} f_\varsigma(y_\rho); \quad \langle\bar{\psi}\psi\rangle = \frac{2}{R^2}\int d\rho\, \rho \langle\bar{\psi}\psi\rangle_\rho$$

- where $x = \frac{p}{T_\rho}$, $y_\rho = \sqrt{x^2 + \frac{m^2}{T_\rho^2}}$.

Tolman Ehrenfest analogy :

- $\mu = 0 \;\rightarrow$ transition is crossover.
- The system can be analyzed perturbatively with respect to $\frac{m_{q;c}}{T_c}$.
- At crossover $\sigma_c^{R,\Omega} \approx \sigma_c^{\infty,0} = 0.45\, g\, f_\pi$.

- In the small mass approximation :

Rotating case :

$$\lambda(\sigma_c^2 - v^2) - h + g^2 \sigma_c N_f (T_\sigma^{\Omega R})^2 \langle \Gamma_\rho^2 \rangle_R \left(1 - 2\varphi_{\Omega R}^2/\pi^2\right) = 0\,.$$

Nonrotating unbounded case :

$$\lambda(\sigma_c^2 - v^2) - h + g^2 \sigma_c N_f (T_\sigma^{\mathrm{nr}})^2 \left(1 - 2\varphi_{nr}^2/\pi^2\right) = 0\,.$$

where, $\langle \Gamma_\rho^2 \rangle_R = \frac{2}{R^2\Omega^2} \ln \Gamma_R$, $\varphi = \tan^{-1} \frac{\sqrt{3(1-L)(1+3L)}}{3L-1}$

Tolman Ehrenfest analogy :

- $\mu = 0 \;\rightarrow$ transition is crossover.
- The system can be analyzed perturbatively with respect to $\frac{m_{q;c}}{T_c}$.
- At crossover $\sigma_c^{R,\Omega} \approx \sigma_c^{\infty,0} = 0.45\, g\, f_\pi$.

- In the small mass approximation:

$$T_\sigma^{\Omega R} = \frac{T_\sigma^{\mathrm{nr}}\sqrt{1-2\varphi_{\mathrm{nr}}^2/\pi^2}}{\sqrt{\langle\Gamma_\rho^2\rangle_R}\sqrt{1-2\varphi_{\Omega R}^2/\pi^2}}.$$

$$\frac{\partial V_L}{\partial L_\pm} = \frac{N_f\varphi_{\Omega R}(T_\sigma^{\Omega R})^4}{2\sin\varphi_{\Omega R}}\left[\left(1-\frac{\varphi_{\Omega R}^2}{\pi^2}\right)\langle\Gamma_\rho^4\rangle_R - \frac{3g^2\sigma_c^2}{4\pi^2(T_\sigma^{\Omega R})^2}\langle\Gamma_\rho^2\rangle_R\right]$$

where, $\langle\Gamma_\rho^2\rangle_R = \frac{2}{R^2\Omega^2}\ln\Gamma_R\,,\quad \varphi = \tan^{-1}\frac{\sqrt{3(1-L)(1+3L)}}{3L-1}$

Tolman Ehrenfest analogy :

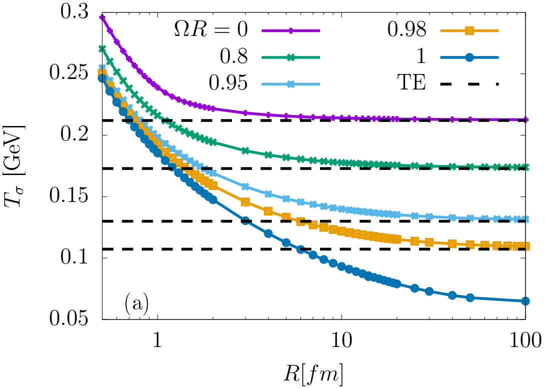

Figure 8: comparison between Tolman-Ehrenfest prediction and numerically estimated transition temperature for PLSM$_q$ model.

- The TE agreement is obtained at high R.

Discussion

- At $T \neq 0,\ \mu \neq 0$ and $\Omega \neq 0$ chiral and deconfinement phase transition is studied in Polyakov enhanced Linear Sigma model with quark degrees of freedom .
- Boundary effects favour the crossover scenario and drags the critical endpoint towards higher chemical potential.
- With increasing rotation the phase transition temperature and critical chemical potential decreases.
- As R increases the ΩR dependency of the critical chemical potential in $T - \mu$ phase diagrams decreases.
- The Tolman-Ehrenfest analogy is investigated for rotating bounded PLSM_q model and we observed a better agreement with increasing R and decreasing ΩR.

Thank You For Your Attention!!